

Dynamical structure of fluid mercury: molecular-dynamics simulations

Kozo Hoshino^{a*}, Shunichiro Tanaka^a and Fuyuki Shimojo^b

^aFaculty of Integrated Arts and Sciences, Hiroshima University, Higashi-Hiroshima 739-8521, Japan

^bDepartment of Physics, Kumamoto University, Kumamoto 860-8555, Japan

Abstract

We have carried out molecular-dynamics simulations for *nonmetallic* fluid mercury in liquid and vapour phases using a Lennard-Jones type effective potential and shown that the structure factors $S(Q)$ and the dynamic structure factors $S(Q, \omega)$ of nonmetallic fluid mercury obtained by our MD simulations are in good agreement with recent x-ray diffraction and inelastic x-ray scattering experiments. We conclude from these results that, though the fluid mercury which shows a metal-nonmetal transition is a ‘*complex*’ fluid, the *nonmetallic* fluid mercury is a relatively ‘*simple*’ liquid, which can be well described by the single density-independent Lennard-Jones type potential.

PACS: 61.20Ja, 61.20Lc

*Corresponding author. Tel.: +81-82-424-6544; fax: +81-82-424-0757

E-mail address: khoshino@hiroshima-u.ac.jp (K. Hoshino)

1. Introduction

Fluid mercury is a complex fluid in the sense that the metallic fluid mercury undergoes a metal-nonmetal (M-NM) transition at about 9 g/cm^3 when the temperature and the pressure of fluid mercury are increased from the triple point to the critical point along the liquid-vapour coexistence curve. Also, the interatomic potential $\phi(r)$ depends strongly on the density, since the fluid mercury is metallic at higher densities and nonmetallic at lower densities. The various physical properties related to the M-NM transition in fluid mercury have been extensively studied and reviewed in the book by Hensel and Warren[1]. Recently, x-ray diffraction and inelastic x-ray scattering (IXS) experiments using synchrotron radiation facilities have provided the static and dynamic structure factors with high resolution [2-5] for fluid mercury in a wide range of density from metallic to nonmetallic. In this paper we are concerned with the static and dynamic structures of *nonmetallic* states of fluid mercury.

As for theoretical studies, first-principles molecular-dynamics simulations have been applied to various liquid metals and alloys; *e.g.* the M-NM transition in fluid mercury was successfully reproduced [6]. It is, however, still difficult to apply the first-principles simulation to large systems even using high performance computers. Under these circumstances the classical MD simulation is suitable and useful to treat large systems, which are necessary when we discuss the long-wavelength density-fluctuations, for instance, in the critical region. For this purpose, it is essentially important that appropriate interatomic potentials $\phi(r)$ are available. Some years ago we [7] have derived $\phi(r)$ by the inverse method, which is based on the modified hypernetted-chain approximation of the integral-equation theory and the molecular-dynamics simulation, from the experimental structure factor $S(Q)$ [8]. We have shown that $\phi(r)$ in the metallic state is quite different from that in the nonmetallic state and that the latter is very similar to the Lennard-Jones (LJ) 6-12 potential. The $\phi(r)$ obtained by the inverse method can be considered as the effective pair potential, since the $\phi(r)$ within the pair potential approximation is chosen so as to reproduce the observed structure factor, which may include the many-body effects beyond the pair potential approximation.

For these reasons we investigate in this paper whether or not the LJ type interatomic potential derived by the inverse method is good enough to describe fluid mercury in the

nonmetallic states. By carrying out the molecular-dynamics (MD) simulations using the LJ type potential, we obtain the static and dynamic structures of ***nonmetallic fluid mercury*** in the liquid as well as in the vapour phases, and compare the results of our simulations with those of the recent x-ray diffraction [2] and the inelastic x-ray scattering [4] experiments.

2. Method of calculation

We have carried out the constant-temperature MD simulations using the Nosé thermostat for *NVT* ensemble with numbers of mercury atoms $N = 864$ and 6912 . We have employed the Lennard-Jones type potential with the potential parameters fitted so as to reproduce the effective pair potential derived by the inverse method for the liquid mercury with 1803K and 6.8 g/cm^3 [7]; the parameters thus obtained are $\varepsilon = 0.104 \text{ eV}$ and $\sigma = 2.79 \text{ \AA}$. Using this interatomic potential the MD simulations have been carried out for five thermodynamic states; the three liquid states ($T(\text{K})$, $\rho (\text{g/cm}^3)$) = $(1273, 11.0)$, $(1673, 9.2)$ and $(1723, 8.8)$, and the two vapour states $(1723, 3.0)$ and $(1673, 2.1)$. We have also studied the metallic state with the density 11.0 g/cm^3 using the LJ potential in order to show that the LJ potential cannot reproduce the observed structure factor of the metallic state of fluid mercury. To study the dynamic properties as well as the static properties we have carried out our simulations for about $200,000$ steps or 960 ps with a time step of 4.8 fs .

3. Results

In Fig.1 we compare the structure factors $S(Q)$ obtained by our simulation with those obtained by the recent x-ray diffraction experiment [2] for five thermodynamic states. The results of our simulation agree very well with the experimental ones except for the state with the density 11.0 g/cm^3 , for such a metallic state the LJ potential is not valid [7] as expected.

In Fig.2 the dynamic structure factors $S(Q, \omega)$ obtained by our MD simulations divided by $S(Q)$ shown in Fig.1 are compared with the recent x-ray inelastic scattering (IXS) experiment [4] for three thermodynamic states. Since the spectrometer resolution was $1.7 - 1.8 \text{ meV}$ in the IXS experiment, we take into account the same resolution when we obtain $S(Q, \omega)$ by the Fourier transformation from the intermediate scattering function $F(Q, t)$ calculated by our MD

simulation. The agreement between the results of our simulation and the IXS experiments is very good, except for the low Q region. The side peak of $S(Q, \omega)$ is not seen in Fig.2, since the smallest Q value 8.7 nm^{-1} for $N=864$ is not small enough. Therefore we have carried out the MD simulation for a larger system with $N=6912$, in which the smallest Q value is about 1 nm^{-1} . In Fig.3 we show the $S(Q, \omega)$ in the long-wavelength region for two liquid states near the M-NM transition region. We can see clear side peaks in these cases.

We can obtain the dispersion relation $\omega(Q)$ from the $S(Q, \omega)$ obtained by our MD simulations. Since the $S(Q, \omega)$ shown in Fig.2 do not show the clear side peak, we calculate the longitudinal current-current correlation function $J_\ell(Q, \omega) = (\omega/Q)^2 S(Q, \omega)$ and we obtain the dispersion relation $\omega(Q)$ from the peak positions of $J_\ell(Q, \omega)$ as a function of ω for various Q values. In the long-wavelength region, we can obtain $\omega(Q)$ from the side peaks of $S(Q, \omega)$ as shown in Fig.3; since the side peaks are sharp, the $\omega(Q)$ obtained from the peak position is almost same as that obtained from $J_\ell(Q, \omega)$. Note that there is no experimental data of $S(Q, \omega)$ for such a small Q value. We show in Fig.4 the $\omega(Q)$ thus obtained. In Fig.4 we also show $\omega_0(Q)$ and $\omega_\ell(Q)$, which are the normalized second and the fourth moments of $S(Q, \omega)$, respectively, defined as follows [9]:

$$\omega_0^2(Q) = \frac{k_B T}{m S(Q)} Q^2,$$

$$\omega_\ell^2(Q) = \frac{3k_B T}{m} Q^2 + \Omega_0^2 - \Omega_Q^2,$$

where

$$\Omega_Q^2 = \frac{n}{m} \int d\mathbf{r} \frac{\partial^2 \phi(r)}{\partial z^2} \exp(-iQz) g(r),$$

$$\Omega_0^2 = \frac{n}{m} \int d\mathbf{r} \frac{\partial^2 \phi(r)}{\partial z^2} g(r),$$

Ω_0 being the Einstein frequency. Since we use the analytic form of the LJ potential for $\phi(r)$, these quantities can be calculated using $g(r)$ obtained by our simulation. The approximate expression for $\omega_\ell^2(Q)$ given by [9]

$$(\omega_\ell^{approx}(Q))^2 = \frac{3k_B T}{m} Q^2 + \Omega_0^2 (1 - j_0(Qr_0) + 2j_2(Qr_0))$$

is sometimes used in the analysis of the experimental data, $j_0(x)$ and $j_2(x)$ being, respectively, the zero-th and second order spherical Bessel functions. To check the validity of this approximate expression, we also show in Fig.4 $\omega_\ell^{\text{approx}}(Q)$ calculated using our Ω_0 .

We can see from Fig.4 that the $\omega(Q)$ locates between $\omega_0(Q)$ and $\omega_\ell(Q)$, *i.e.* $\omega_0(Q) < \omega(Q) < \omega_\ell(Q)$, and that $\omega_\ell^{\text{approx}}(Q)$ is a good approximation for $\omega_\ell(Q)$. In Fig.4 we show the straight dotted lines corresponding to the experimental sound velocities v_s [10] for each density of fluid mercury. The dispersion curves $\omega(Q)$ in the long-wavelength region is always larger than the straight lines $\omega = v_s Q$, which is the so-called positive dispersion and suggests a larger sound velocity. The amount of deviation from the straight lines is large around the density of 9.0 g/cm³, which corresponds to the density where the M-NM transition occurs, and the deviation is smaller for the mercury vapour.

4. Discussion

As is shown in Fig.1 the LJ type potential determined so as to reproduce the structure factor $S(k)$ of liquid mercury with 1803K and 6.8 g/cm³ is able to describe the structure of nonmetallic fluid mercury for a wide range of density. Moreover, as is shown in Fig.2, the dynamic structure factors $S(k, \omega)$ can also be well reproduced by the MD simulation using the LJ type potential.

The dispersion relations $\omega(Q)$ obtained by our MD simulations show the positive dispersion and their density dependence is consistent with the recent IXS and inelastic neutron scattering (INS) experiments [5,11]; Ishikawa *et al.* [5] have found by the IXS experiment that a large deviation, *i.e.* a large sound velocity, can be obtained near the M-NM transition region and they attributed the ‘fast sound’ to the large fluctuation of the pressure due to the M-NM transition. Bove *et al.* [11] found that the sound velocity of metallic liquid mercury obtained by the INS experiment is much larger than that obtained by the ultrasonic experiment [10].

These results show that the static and dynamic structures of *nonmetallic* fluid mercury can be well reproduced by the single density-independent LJ type potential and suggest that the nonmetallic fluid mercury can be said to be a simple liquid like a liquid argon, though the metallic liquid mercury is a complex liquid with density-dependent pair potential. This is

understandable since the mercury atom has a closed-shell electronic structure.

We can investigate the static and dynamic structures of fluid mercury in the supercritical region, where the long-wavelength density-fluctuation plays an important role, by a large-scale MD simulation using the LJ type potential, the validity of which for the nonmetallic fluid mercury is confirmed in this paper. Such a study is now in progress.

5. Conclusion

We have shown in this paper that: (1)The static structures such as the structure factors $S(Q)$ of nonmetallic fluid mercury obtained by our MD simulations are in good agreement with the x-ray diffraction experiments [2]. (2)The dynamic structure factors $S(Q, \omega)$ calculated by the Fourier transform of the intermediate scattering functions $F(Q, t)$ obtained by our MD simulations agree well with those of the recent inelastic x-ray scattering experiments [4].

These results suggest that the static and dynamic structures of the nonmetallic fluid mercury in the liquid and vapour phases as well as in the supercritical region can be well described by the single density-independent LJ type potential. We can conclude from these results that, the ***nonmetallic*** fluid mercury is a relatively ‘***simple***’ liquid, though the fluid mercury which shows the M-NM transition is a ‘***complex***’ fluid.

Acknowledgments

We are grateful to Professor M. Inui, Professor K. Tamura and Mr. D. Ishikawa for providing us with their experimental data and useful discussions. This work was supported by a Grant-in Aid for Scientific Research from the Ministry of Education, Science, Sports and Culture, Japan.

References

- [1] F. Hensel and W.W. Warren, Jr., *Fluid Metals* (Princeton University Press, 1999)
- [2] M. Inui, X. Hong and K. Tamura, Phys. Rev. **B68** (2003) 094108.
- [3] S. Hosokawa, H. Sinn, F. Hensel, A. Alatas, E.E. Alp and W.-C. Pilgrim, J. Non-Cryst. Solids **312-314** (2002) 163.
- [4] D. Ishikawa, M. Inui, K. Matsuda, K. Tamura, A.Q.R. Baron, S. Tsutsui, Y. Tanaka and

- T. Ishikawa, J. Phys.: Condens. Matter **16** (2004) L45.
- [5] D. Ishikawa, M. Inui, K. Matsuda, K. Tamura, S. Tsutsui and A.Q.R. Baron, Phys. Rev. Lett, **93** (2004) 097801.
- [6] G. Kresse and J. Hafner, Phys. Rev. B**55** (1997) 7539.
- [7] S. Muneyoshi, F. Shimojo and K. Hoshino, J. Phys.: Condens. Matter **10** (1998) 4963.
- [8] K. Tamura and S. Hosokawa, J. Phys.: Condens. Matter **6** (1994) 419.
- [9] see, e.g. U. Balucani and M. Zoppi, *Dynamics of the Liquid State* (Oxford University Press, 1994)
- [10] M. Yao, K. Okada, T. Aoki and H. Endo, J. Non-Cryst. Solids **205-207** (1996) 274.
- [11] L.E. Bove, F. Sachetti, C. Petrillo, B. Dorner, F. Formisano, M. Sampoli and F. Barocchi, Phil. Mag. **B82** (2002) 365.

Figure Captions

Fig.1 The structure factors $S(Q)$ obtained by our MD simulations (solid lines) are compared with experimental results (dots)[2] for five thermodynamic states of fluid mercury. The values of density in parentheses correspond to those where $S(Q)$ were measured by x-ray diffraction experiments [2].

Fig.2 The dynamic structure factors $S(Q, \omega)$ divided by $S(Q)$ for three thermodynamic states of fluid mercury. The results of our MD simulations (solid lines) are compared with those of inelastic x-ray scattering experiments (dots)[4].

Fig.3 The normalized dynamic structure factors $S(Q, \omega)/S(Q)$ in the long-wavelength region obtained by our MD simulations for two thermodynamic states of fluid mercury.

Fig.4 The dispersion relations $\omega(Q)$ as a function of Q for four thermodynamic states of fluid mercury. The results of our MD simulation are shown by open circles obtained from the peak position of $J_\ell(Q, \omega)$ and by diamonds obtained from the side peaks of $S(Q, \omega)$. The straight dotted lines show $\omega = v_s Q$, where v_s is the observed sound

velocity obtained by the ultrasonic experiment [10]. The normalized second and the fourth moments, $\omega_0(Q)$ and $\omega_\ell(Q)$, defined in the text are also shown by long-dashed lines and solid lines, respectively. The approximate form $\omega_\ell^{approx}(Q)$ for $\omega_\ell(Q)$ is also shown by short-dashed lines.

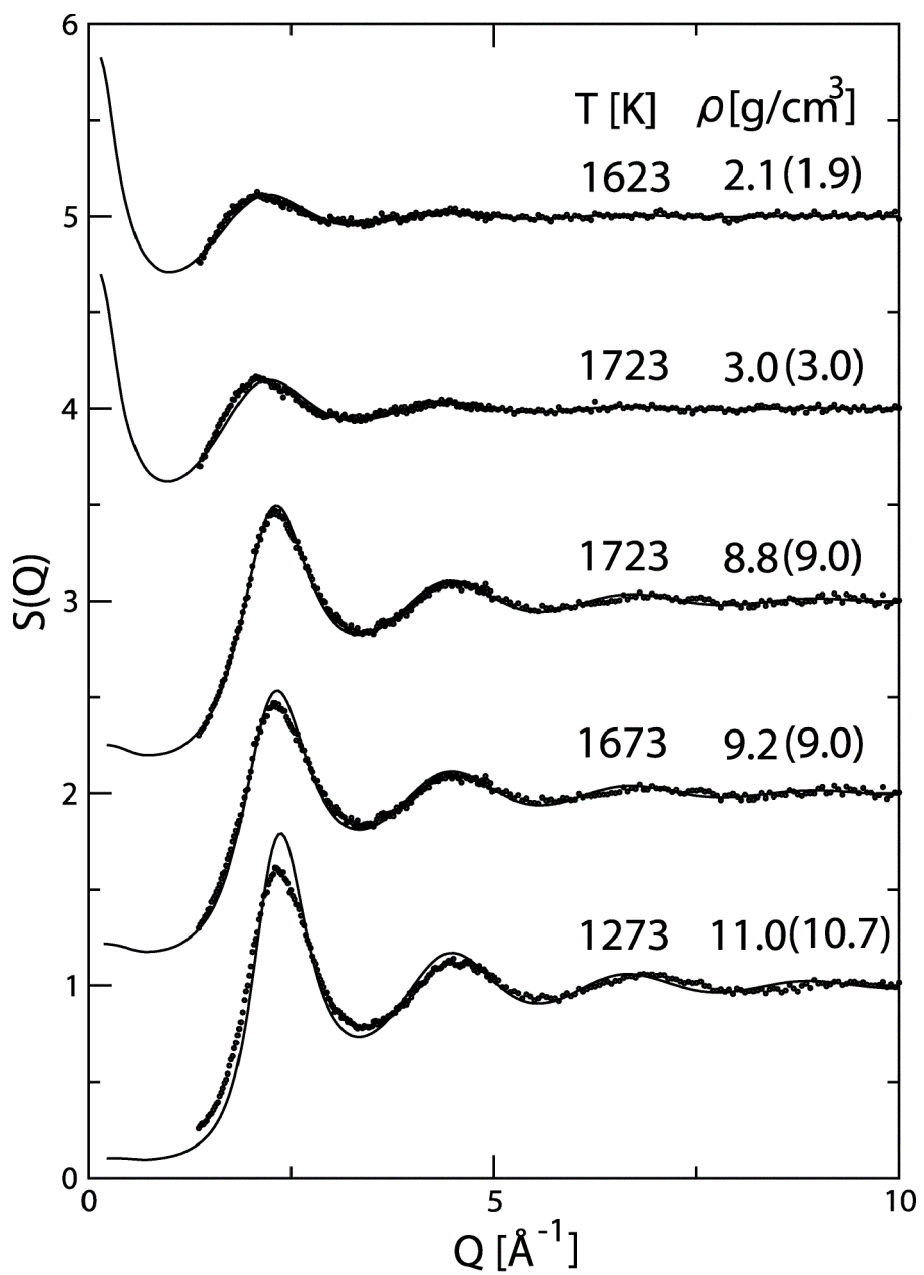


Fig. 1 Hoshino et al.

$T=1673[K]$, $\rho=9.2[g/cm^3]$ $T=1723[K]$, $\rho=3.0[g/cm^3]$ $T=1623[K]$, $\rho=2.1[g/cm^3]$

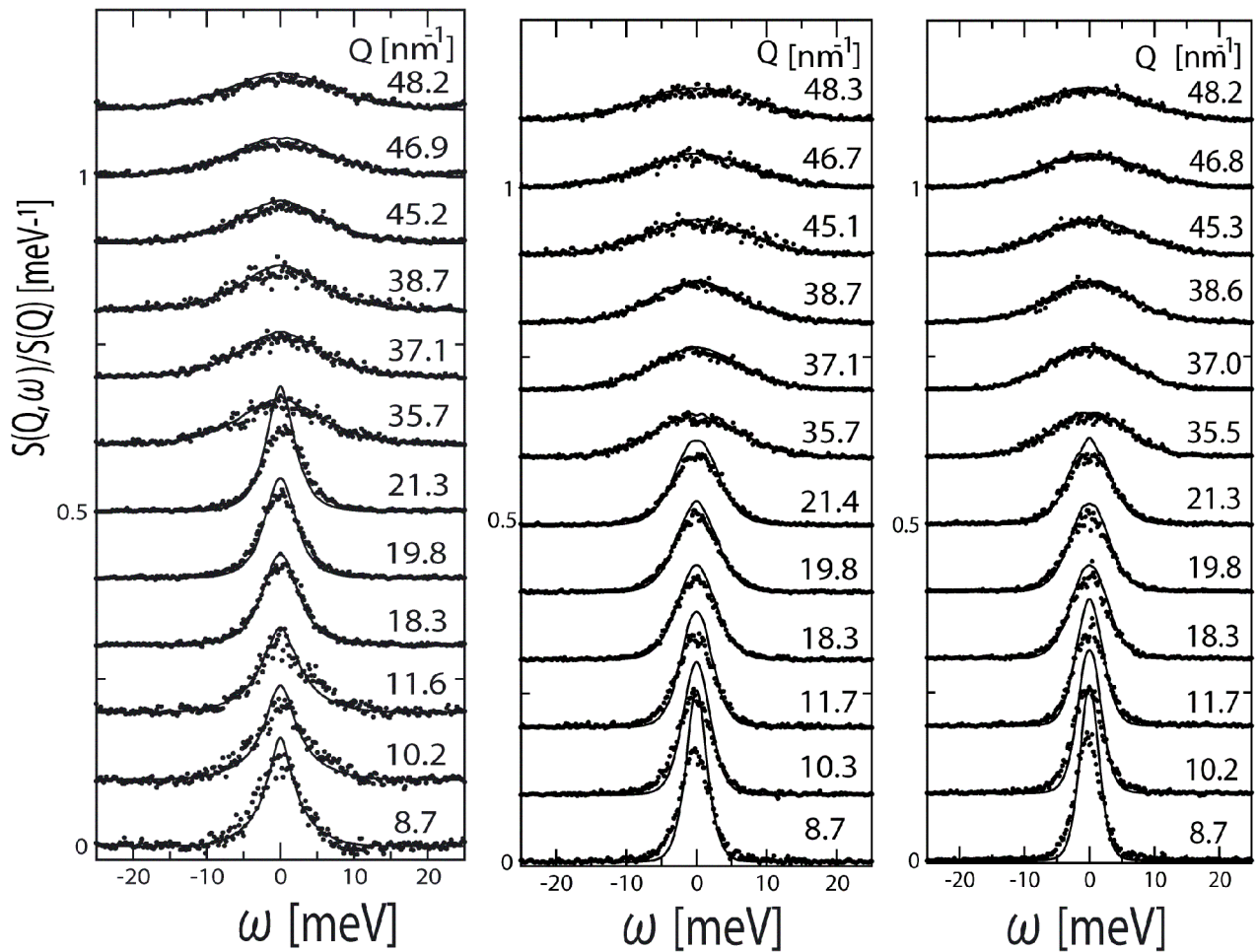


Fig. 2 Hoshino et al.

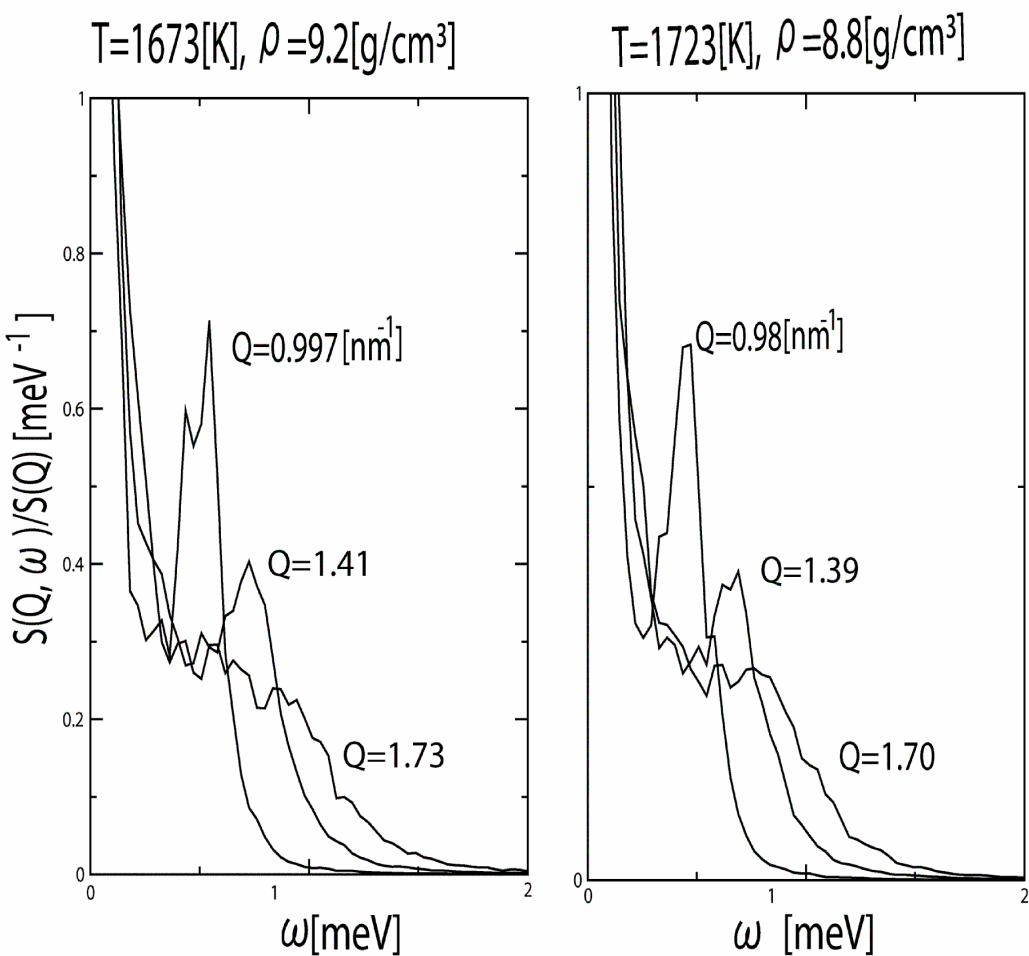


Fig. 3 Hoshino et al.

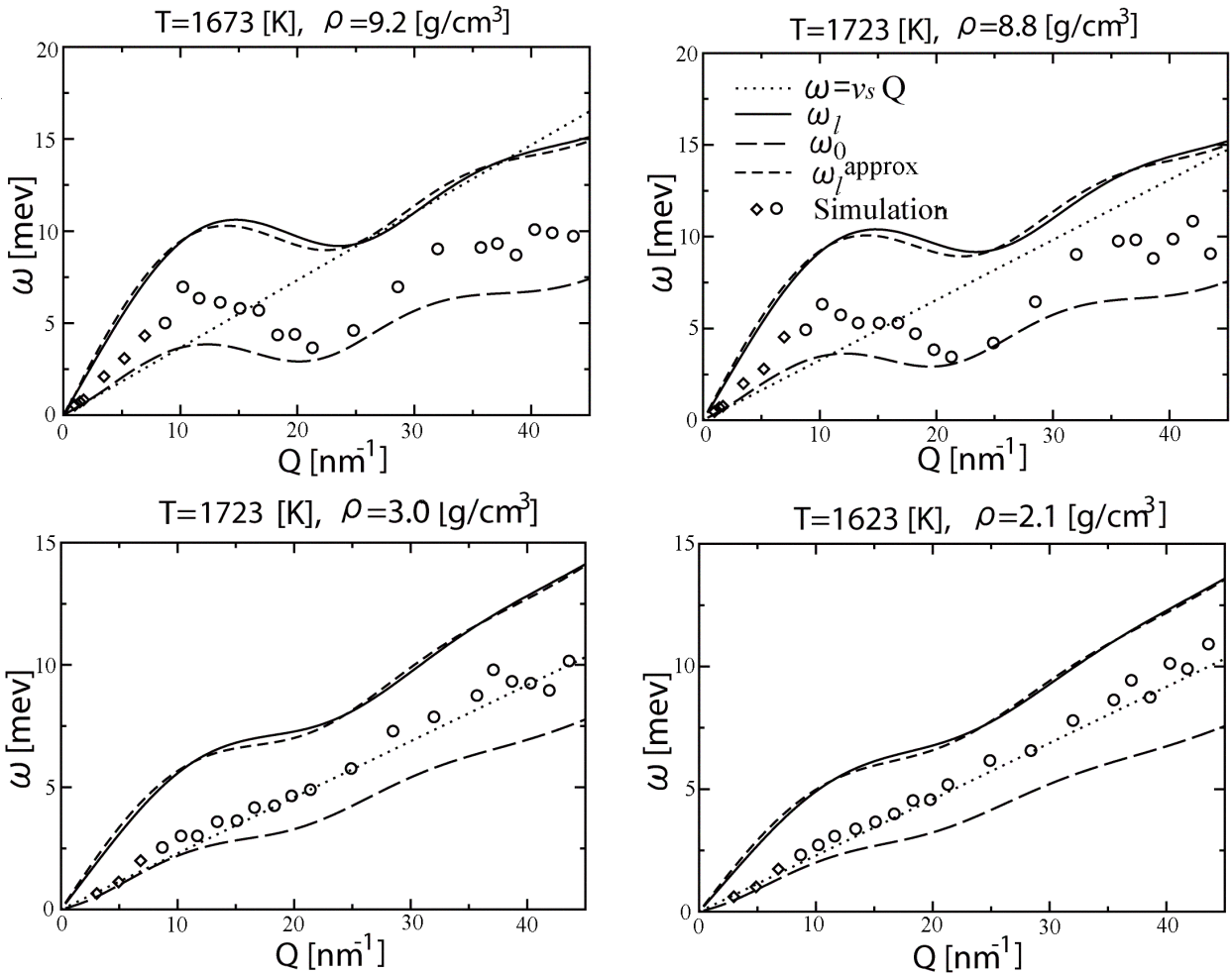


Fig. 4 Hoshino et al.